COO-4878-1

SOLAR-HEATED-AIR TURBINE GENERATING SYSTEMS

Philip O. Jarvinen*

M.I.T. Lincoln Laboratory

CONF-750812--14

Abstract

The feasibility of large-scale solar electrical power generation using open cycle heated air turbines in conjunction with a tower-mounted, pressurized, central receiver/heliostat system is investigated. Such a system requires no cooling towers and may be sited away from cooling water supplies. A regenerative open cycle/solar gas turbine approach is chosen since it offers higher overall thermal efficiency than a simple cycle and because peak efficiency is achieved at a pressure ratio of about 4 to 1; which minimizes design considerations of the pressurized receiver. The feasibility of the heated air receiver is demonstrated and structural design, heat transfer and efficiency aspects of a windowless cavity receiver which provides 1800°F heated air are discussed. The capabilities of the M.I.T. Lincoln Laboratory solar simulator and the U. S. Army 35 KW thermal W. S. M. R. and the 1000 KW thermal C. N. R. S. solar furnaces for testing heated air receivers are explored. It is concluded that a central receiver solar thermal heated air gas turbine power plant is feasible and that future efforts should be directed at the development of the most effective receiver possible in order to minimize heliostat collector field area and system cost.

Solar-Heated Air Concept

System analysis and component design leading to an early solar thermal/steam power plant demonstration for the production of electrical energy are now underway under the sponsorship of ERDA/NSF. The preferred preliminary design configuration utilizes a tower receiver(s)[1,2] that produces high pressure, 950°F superheated steam for turbine generator operation. However, water availability appears to be a major problem for such a system.

Solar power stations will be sited in areas of maximum solar insolation; areas that correspond to the arid sections of the world. Most solar thermal/steam power plants require substantial amounts of water that are lost in the operation of wet cooling towers for system cooling. The alternative to wet cooling towers: namely dry cooling towers, is quite costly. In fact, proposed 1000-MW units require cooling-tower water-flow rates in the range of 10,000 to 20,000 gallons-per-minute. The requirements for substantial amounts of water at solar generating sites limit the developed technology to certain restricted parts of solar intensive regions.

Heated-air solar-power generation systems are a viable alternative to steam generator units, but have not received significant study to date. Heated-air systems demand development since the advantages of such systems are manyfold, the chief of which include (a) elimination of the need for cooling water supplies, (b) use of air as the heat-transfer fluid, a universally available, no-cost fluid, and (c) operation at temperatures thousands of degrees hotter than that allowed by solar-steam systems.

Heated-air systems may be developed in the same time period as proposed steam generation units. A 1-MW, thermal-heated-air demonstration unit could be built for test in the French solar energy facility in Odeillo within two years, and a 10-MW unit could be built and tested within five years. However, this schedule may be achieved only if sufficient funding and priority are allocated to the approach.

One concept which offers early demonstration of solar-heated-air electrical power generation and which will be discussed in the following paper is that of a central tower, heated-air receiver that supplies heated fluid to a gas turbine power plant operating in an open-Brayton-cycle type mode (Fig. 1). The gas turbine electrical power station is located near the base of the central tower; upon which is mounted the heated air receiver. The field of heliostats about the tower redirects the incident solar flux to the receiver where it is absorbed and used to heat the working fluid; in this case, a gas. The gas flow, initially compressed on the ground, is ducted to the receiver and then back down to the turbine section on the ground. The heated-air receiver of the solar power generator replaces the combustion chamber of the ordinary gas turbine. The pressurized heated air receiver is designed to provide turbine inlet temperatures of 1800°F; as currently employed in gas turbine equipment. To achieve gas temperatures of this magnitude, the receiver utilizes a multiple cavity approach and each cavity is constructed from ceramic materials which have the

*M.I.T. Lincoln Laboratory, Lexington, Mass. 02173

This work was sponsored by the Department of the Air Force and the M.I.T. Energy Laboratory.

PREPARED FOR 10th INTERSOCIETY ENERGY CONVERSION AND ENGINEERING CONF. U OF DELAWARE, NEWARK DELAWARE AUG 17-22, 1975.

DISCLAIMER

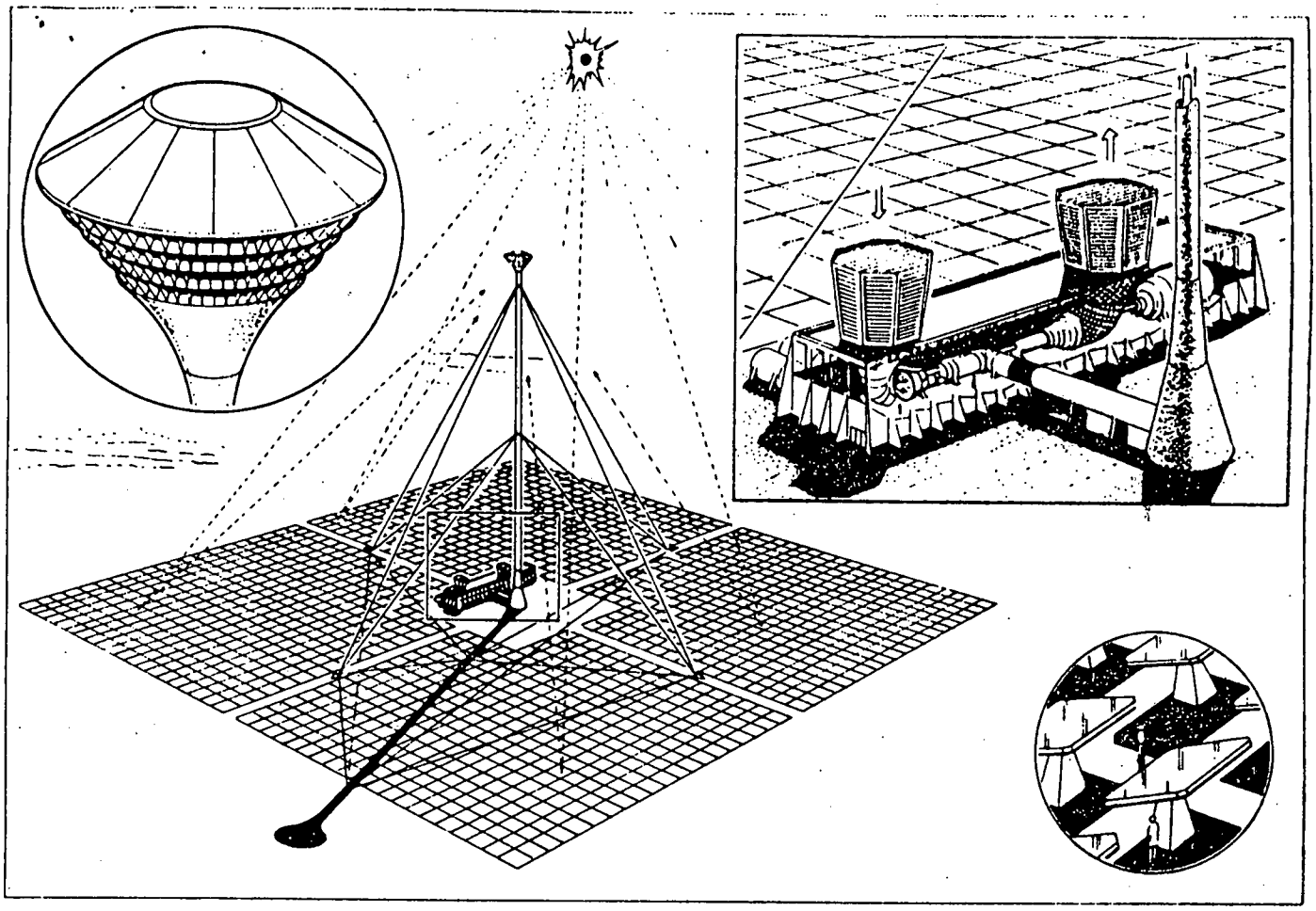

Fig. 1. Artist's rendering of proposed solar-heated-air electrical power generation plant.

capability of continuous operation at maximum temperatures as high as 3000°F. Though a ground based gas turbine generator unit is shown in Fig. 1, it may be possible, in some applications, to mount such a unit on the tower in combination with the receiver.

Solar-Powered Brayton Cycle

The basic gas-turbine cycle is a Brayton cycle consisting of adiabatic compression, constant pressure heating, and adiabatic expansion (Fig. 2). In a simple open Brayton cycle, the expanded flow (Point 4) is exhausted to the atmosphere. There is no recirculation of working medium within the structural confines of the power plant; the inlet and exhaust being open to the atmosphere (Fig. 3). By adding a regenerator (Fig. 4) to recover heat from the turbine exhaust, the efficiency is improved. The open cycle offers the advantage of a simple control and sealing system and can be designed for high power-to-weight ratios and for operation without cooling water. A solar-powered gas turbine results from the replacement of the fuel combustor with a solar-heated-air receiver.

The operating efficiencies of solar-powered gas turbine units may be obtained by analogy with the efficiencies of fuel-fired gas turbine units. At a turbine inlet temperature of 1800°F, present day simple open-cycle gas turbine generator units,[3] for

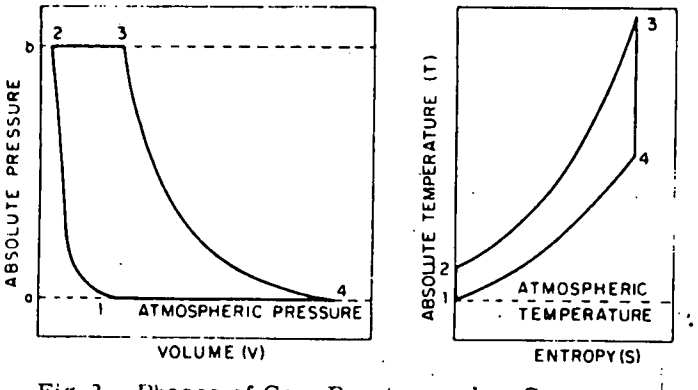

Fig. 2. Phases of Gen. Brayton cycle: Compression 1-2; addition of heat at constant pressure, 2-3; expansion, 3-4; heat abstraction, 4-1.

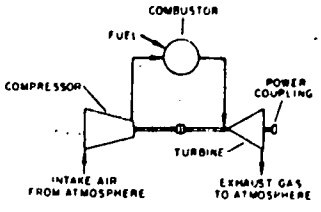

Fig. 3. Simple open-cycle gas turbine.

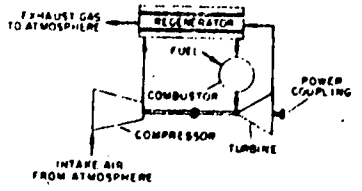

Fig. 4. Open-cycle gas turbine with regeneration.

standby generation, have an overall efficiency of about thirty percent. Cycle analyses[4] of a regenerative gas turbine are noted in Fig. 5 and show that a regenerative solar gas turbine unit with a turbine inlet temperature of 1800°F and ambient inlet temperature of 100°F (T_{03}/T_{01} = 4) achieves maximum efficiency (η = 0.44) at a pressure ratio of about 4. Similar calculations for a simple open cycle show that the maximum efficiency (η = 0.33) is achieved at a much higher pressure ratio; about 16. Thus, for a temperature ratio of four, the regenerative gas turbine cycle gives a peak thermal efficiency 10 points higher than the simple cycle with the additional advantage that it is achieved at a compression ratio four times less. In view of the importance of obtaining high thermal efficiency, the choice of cycle seems to fall conclusively on the regenerator cycle.

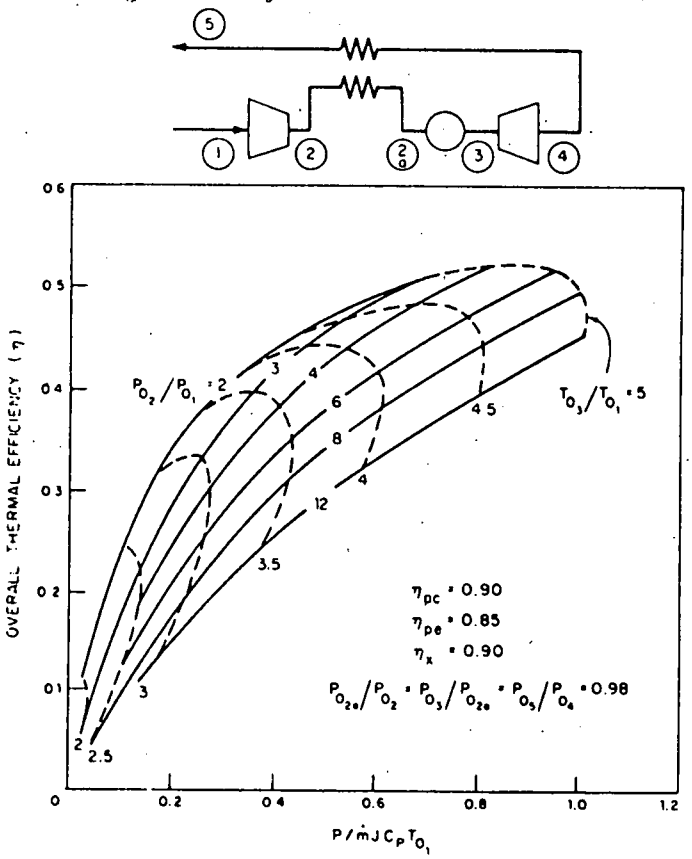

Fig. 5. Regenerate gas turbine cycle analysis.

Collector Field Performance

The studies performed by the University of Houston/Mc Donnell-Douglas[1] and Martin-Marietta[2] of tower receiver/optical transmission solar steam power systems provide substantial information on heliostat/tower/receiver trade-offs. Design aspects, such as the orientation and distribution of mirrors in a heliostat field, the angle of incidence of the sun on the mirrors, shading and blocking of adjacent mirrors, desirable receiver shapes and the projection of incident concentrated sunlight beams on receivers are known from these works.

The substantial amount of available information[1] which exists on the performance of the heliostat/central tower approach allows an approximate model to be developed which may be used to determine heliostate field size and tower height (within two percent of the computer calculations of Ref. 1) for a given receiver thermal handling capacity. The resulting thermal capacity formula, for the geometry shown in Figure 6, is:

$$C = K_1K_2K_3K_4K_5 \text{ (solar insolation) (ground area A)} \quad (1)$$

where K_1 = cos i = projection of ground area, A, perpendicular to sun ray

K_2 = heliostat ground coverage.

K_3 = tracking efficiency of heliostat field (see Fig. 8)

K_4 = heliostat reflectivity

K_5 = thermal absorption efficiency of receiver.

While that for tower height, in meters, is

$$h' = .167\sqrt{A(m^2)} \quad (2)$$

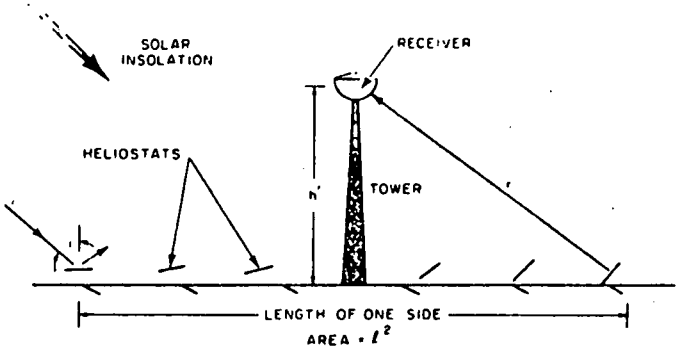

Fig. 6. Heliostat/receiver geometry.

Approximate values for required field area and tower height as a function of thermal capacity are shown in Figure 7 for a heliostat field/central receiver system designed for winter operation at 35° latitude. For example, a 200MWt* capacity system would have a tower height of 173 meters, would cover a ground area of 1.65 KM^2 and have a side length of about 1.3 KM.

The tracking efficiency was determined from Fig. 8 (reproduced from Ref. 5). Aerospace Corporation[5] was able to compress the computer calculations of the University of Houston for heliostat field tracking efficiencies for an entire year to the single plot shown in Fig. 8. Tracking efficiency includes col-

* Megawatt thermal

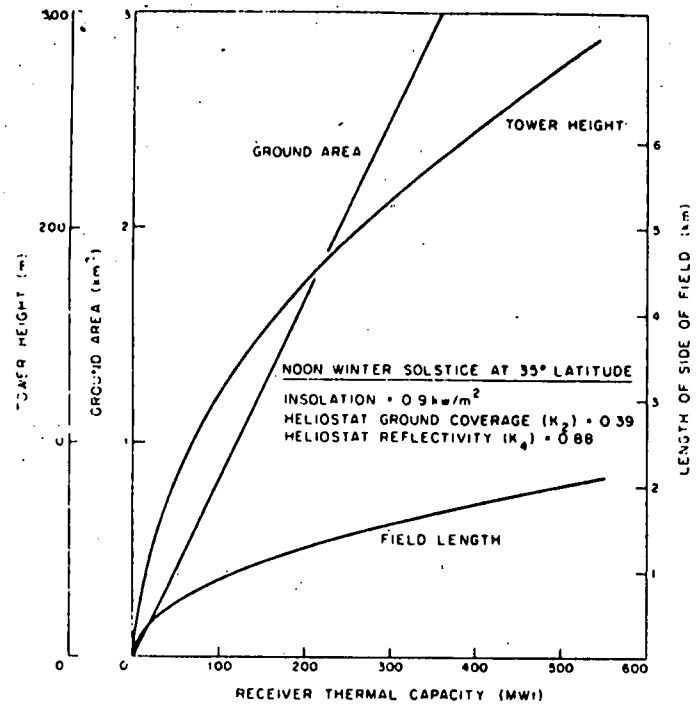

Fig. 7. Field area and tower height vs thermal capacity.

lector losses due to relative orientation of the heliostats with respect to the sun's rays and the effects of shading and blocking by adjacent heliostats. This tracking efficiency data, in conjunction with the approximate model noted above, allows the thermal input to a central receiver to be calculated quickly and accurately at any season of the year or time of the day.

Heliostat Image Sizes at the Receiver

Manufacturing considerations limit the size of ceramic elements that may be used in heated air receivers to a maximum diameter of about three meters. The question arises as to whether there are applications in which a single three-meter diameter receiver is adequate or do most applications require a larger receiver; constructed by assembling together a number of the ceramic elements. Since receiver size is dictated, to a large extent, by the image size of an individual heliostat at the receiver, a study of image sizes is in order. However, before calculating image sizes, a brief review of two possible heliostate field/tower systems[1,2] will be made to illustrate their differences.

References 1 and 2 differ significantly in their solution to heliostat field/receiver designs. Reference 1 considers a centrally-located receiver which accepts reflected sunlight from all azimuthal directions and uses movable flat-plate heliostats. Reference 2's solution is to break up the large heliostat field into several smaller sub-fields, each with their own receiver mounted on a tower which is considerably shorter than

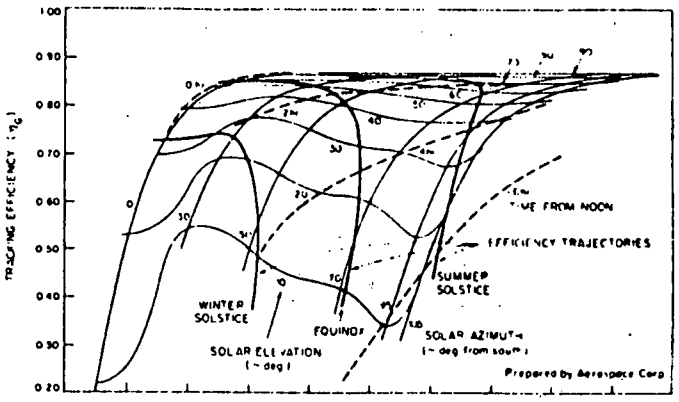

Fig. 8. Central receiver tracking efficiency.[5]

the single centrally-located tower. Curved heliostat mirrors are used in this approach to produce a smaller image size at the receiver than would be obtained from flat heliostat reflectors.

Image sizes of individual heliostats at the receiver depend on surface and aiming errors, the heliostat size chosen and optical effects such as spherical aberation (in curved heliostats). The image size for a flat mirror, perfectly aimed, is given by the formula:

$$D_{i_F} = D_s + (\text{sun angle})\, r + (\text{surface error})\, r$$

where D_s = heliostat size

r = distance from heliostat to receiver

and curved mirrors (formed by warping flat sheets of glass) have been found[2] empirically to produce image sizes given by the formula

$$D_{i_C} = 2\,(\text{sun angle})\, r$$

Image sizes have been calculated as a function of r, the heliostat to receiver distance, for flat and curved mirrors and the results are shown in Fig. 9.

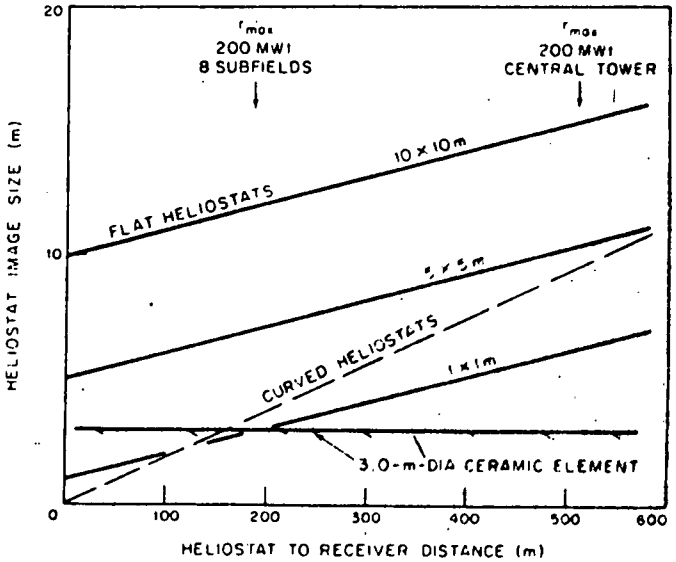

Fig. 9. Image sizes for curved and flat heliostats.

A 200MWt central tower system with flat heliostats in the size range from 1 to 10 meters will have maximum image sizes of 6 to 16 meters while a multiple sub-field system of the same total capacity with curved mirrors will have a maximum image size of only 3 meters. Thus we see that image sizes for a 200MWt central tower are large in comparison to a three-meter ceramic element and such a receiver would of necessity have to be built by assembling a number of the ceramic receiver elements together while a three-meter ceramic element is sufficiently large to meet the needs of a 200MWt multiple field, multiple receiver system.

Solar Flux Distribution and Magnitude at the Receiver

The quality of the reflected energy at the receiver must be known in order to design the receiver. The beam of energy is the summation of the contributions from each of the numerous heliostats. The contributions of each heliostat depends on its location in the field along with other factors such as the latitude, season, time of the day and blockage of adjacent heliostats. Luckily, computer programs and computer-generated information are available[1] to describe this complex situation. Published results from Reference 1 will be used to answer questions such as:

1. What is a practical maximum concentration ratio (number of suns) for a central tower/heliostat field?
2. What is the distribution of flux, in azimuth and elevation, at a central tower receiver?
3. How is the peak flux related to the average flux over the receiver?

The variation of flux along north and south facing meridians (i.e., variation with elevation) on a 20-m diameter hemispherical receiver[1] in a 1.8 KM × 1.8 KM collector field is shown in Fig. 10. The results are presented in terms of a dimensionless heat flux ξ and are plotted versus depth below the top of the hemisphere. The dimensionless flux ξ is[1] the ratio of the heat flux on the receiver to the product of the normal solar constant, mirror reflectivity and receiver absorptivity:

$$\text{i.e.,} \quad \xi = \frac{q''}{E_s \xi_m \alpha A}$$

These calculations show that present central tower/flat heliostat systems are capable of achieving peak concentration ratios of at least 2000, the azimuthal distribution of flux around a central tower varies slowly and may be made nearly constant by tailoring the heliostat field, the variation of flux vertically in the beam or on the receiver is roughly of gaussian form and the average flux is about 73 percent of the maximum flux in

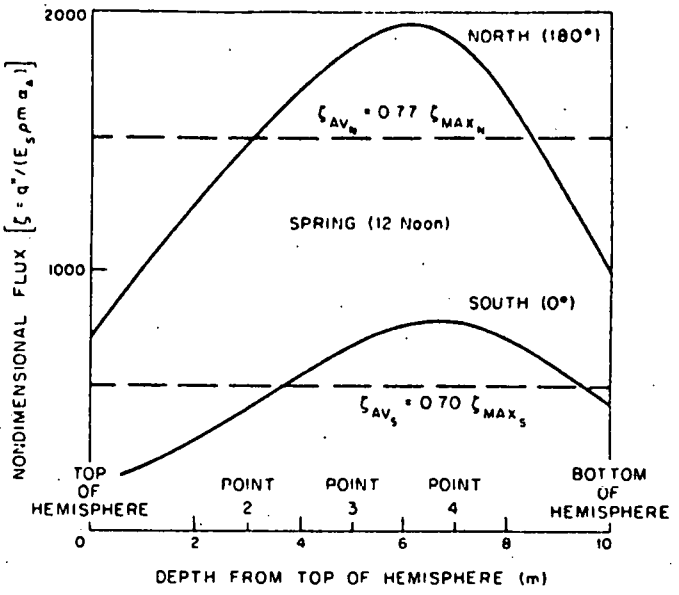

Fig. 10. Variation of flux along north and south facing meridians of the hemispherical receiver.

the same vertical plane. Reference 1 noted that a practical utilization limit for a steam receiver is only about 1000 suns and a new heliostat aiming strategy was instituted to lower the flux to this level.

Receiver Configurations

A variety of receiver configurations are possible which can provide heated air at 1800°F to the power turbine on the ground. Several examples of surface and cavity central receivers constructed from ceramic tubes and domes are shown in Fig. 11. In the tube approach, sunlight is absorbed on the outside of the tubes and the heat is conducted through the wall to pressurized air flowing through the tube. In the dome approach, the dome is faced convex side toward the internal pressure and carries the pressure loads by going into overall compression; in the same manner as windows for undersea craft. Heat is conducted through the dome wall and absorbed into the airflow through an impingement heat transfer scheme which utilizes numerous impinging air jets directed at the

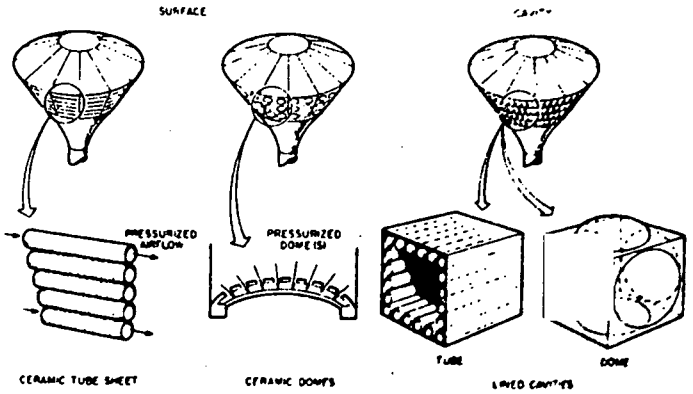

Fig. 11. Windowed or windowless central tower/heated-air receiver configurations.

convex side of the dome (Figure 12 and Figure 15). Small sub-field receivers would be constructed from a single dome or from a limited number of tubes.

The overall feasibility of heated air receivers will now be demonstrated by considering structural design, heat transfer, operating temperature and energy balance aspects of a cavity receiver segment. The cavity domed receiver segment, Fig. 12, will be selected for analysis. In this configuration, sunlight, admitted through the open end of the cavity, heats the five ceramic domes forming the interior walls of the cavity. Impinging jets on the backside of each dome carry the heat away. The cavity shown in Fig. 12 has a depth to width ratio of unity but the domed approach may also be used with deeper cavity designs as well. Since the intent of the analysis is only to demonstrate concept feasibility, no attempt is made to find an optimum receiver.

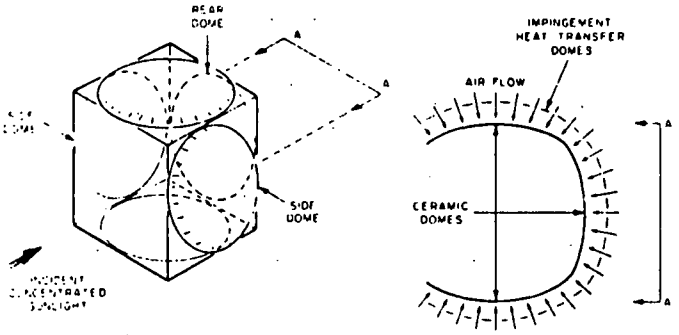

Fig. 12. Multiple-dome/capacity receiver.

Dome Structural Design

Buckling of the dome under pressure loads is selected as the structural design criterion. This phenomena was studied in Reference 6 where it was shown that the buckling of spherical domes is described by the formula

$$\frac{P}{E} = \frac{0.8}{\sqrt{1-\nu^2}}\left(t/R\right)^2 \qquad (1)$$

where P is the design pressure (which of course is appropriately factored upwards for safety), E is the modulus of elasticity, ν is Poisson's ratio and t and R are the thickness and radius of curvature of the dome, respectively. Equation (1) holds for spherical shell segments spanning a chordal distance, b, (see Fig. 13). For the geometry shown, the distance b and the height h are given by the equations:

$$b = 2R\sin\theta \qquad (2)$$

and $$h = R(1-\cos\theta) \qquad (3)$$

The thickness of a silicon carbide dome, for a turbine pressure ratio of four and a factor of safety of three, has been calculated for chordal distances to 120 in. and various values of height to span ratio,

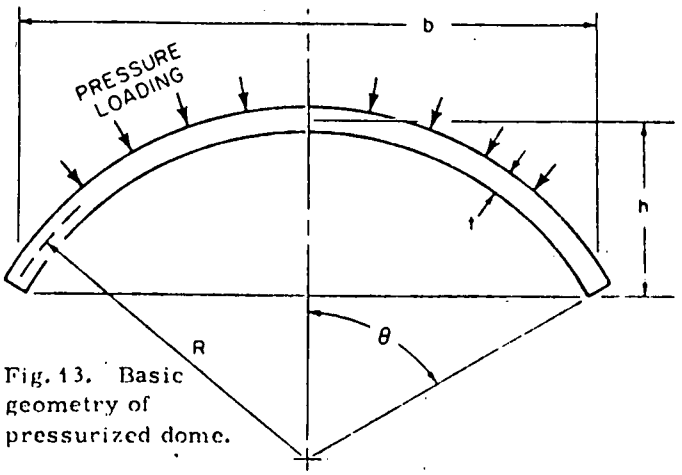

Fig. 13. Basic geometry of pressurized dome.

$h/_b$, and the results are shown in Fig. 14. Though the thinnest shell will be attained with a full hemisphere ($\theta = 90°$, $h/_b = 0.5$), a spherical shell segment with $h/_b = 0.20$ will be selected for the present receiver since it is nearly as effective as a hemispherical dome (0.20 inch thickness versus 0.14 inch thickness for a hemispherical dome of 3 meter span) and its lower dome height for a given span eases the packing of adjacent cavities in a multiple cavity receiver. Thickness requirements for flat and cylindrical shell receivers are also noted in Fig. 14 and a comparison of these receiver types with the preferred spherical shell shows that their thicknesses (and weights) are one order of magnitude greater, at the same receiver operating pressure ratio.

Silicon carbide was chosen for the dome material because it can be operated continuously at temperatures as high as 3000°F without degradation in an oxidizing atmosphere and because it has excellent thermal shock properties. Material properties assumed in the calculations are listed in Table 1 along with other pertinent information:

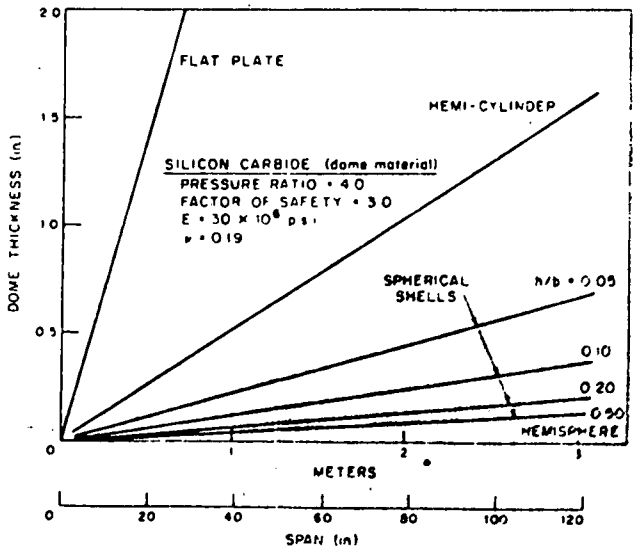

Fig. 14. Dome thickness.

Table 1. Silicon Carbide Properties

E = Modulus of elasticity = 30×10^6 psi

ν = Poisson's ratio = 0.19

T_{op} = Continuous operating temperature = 3000°F

Crushing strength = 100,000 psi

Rupture strength

Room temperature = 14,000 – 18,000 psi

2700°F (1500°C) = 18,000 – 22,000 psi

Thermal Conductivity = 11 BTU/hr ft^2 °F/ft (3000°F)

ϵ_λ = Normal spectral emittance = 0.70

(λ = .665 μ, T = 3000°F)

ϵ = Emissivity = 0.90 (3000°F)

Receiver Heat Transfer

An impingement heat transfer technique will be used to cool the ceramic dome and heat the air supply to the desired temperature. Impingement heat transfer techniques have been studied and the following correlation formula has been developed to describe the data

$$S_t = \frac{h}{GC_p} = 0.30\,(GD/\mu)^{-0.28}\,(x_n/D)^{0.875} \qquad (4)$$

which is applicable in the range

$$1 \leq x_n/D \leq 6.5$$

and

$$10 \leq (GD/\mu) \leq 1000$$

and where

h = heat transfer coefficient

G = mass flow rate = ρV

D = hole diameter

μ = viscosity of heat transfer fluid

C_p = specific heat of heat transfer fluid

x_n = inter hole spacing (See Figure 15)

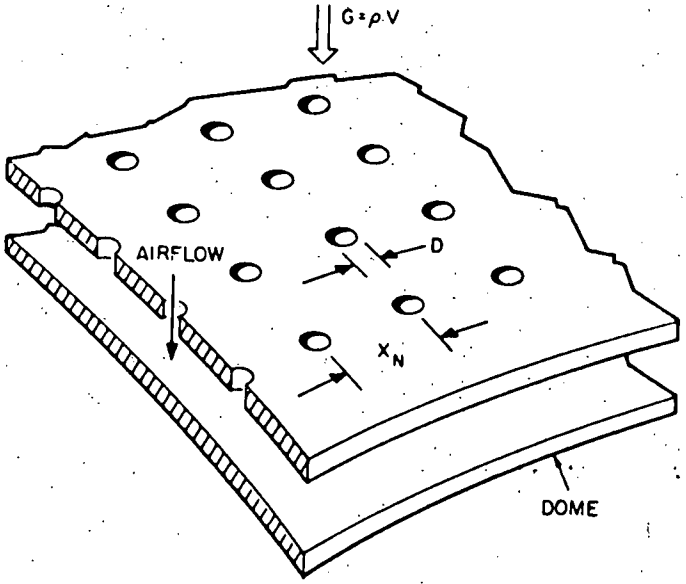

Fig. 15. Impingement heat-transfer geometry.

The pressure drop through the impingement device is proportional to

$$\Delta P \propto G^2\left(\frac{x_n}{D}\right)^4$$

and the pumping power $Q\Delta P$ is proportional to

$$Q\Delta P \propto G^3\left(\frac{x_n}{D}\right)^4$$

The heat transfer coefficient variation as a function of impingement hole diameter is shown in Figure 16 for a fixed mass flow rate and three interhole to hole diameter ratios. The pressure drops needed to achieve the heat transfer coefficients are also noted in Figure 16. Impingement heat transfer is three to six times more effective than conventional heat transfer for the same pressure drop. The results shown in Figure 16 do not consider spent air effects on heat transfer but it is felt that such effects may be avoided through careful design of the impingement system.

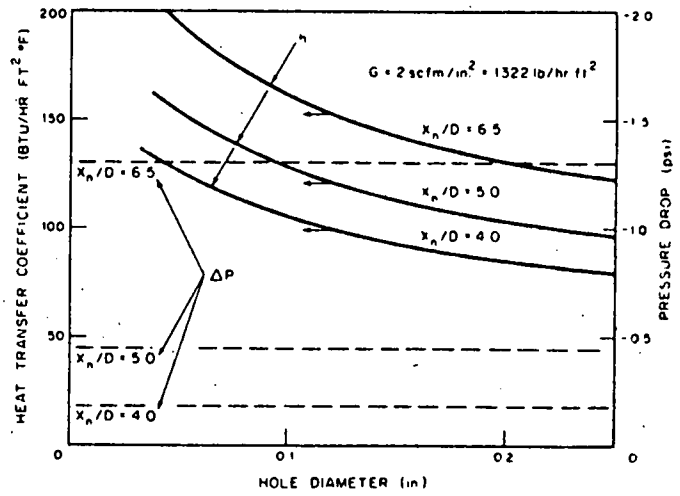

Fig. 16. Impingement heat-transfer coefficients and pressure drop.

Receiver Energy Balance

The windowless five dome cavity receiver segment (Fig. 12) with depth, d, to width, w, ratio or unity and constructed from silicon carbide with ϵ = 0.90 will act as a black body radiator with effective emmissivity or unity and have a radiative heat loss rate of

$$q_{loss} = F_{1R2}\,\sigma\,T_{eq}^4\,A_{aperture} \qquad (5)$$

where F_{1R2} = cavity radiation viewfactor

= 0.52 for cavity with d/w = 1.0 (Ref. 7)

If heat is not actively removed from the cavity, an equilibrium temperature is reached where the incident flux is equal to the reradiated flux. For example, the cavity (Figure 12), d/w = 1.0 will have an equilibrium cavity temperature of 2350°F under an input of 150

REPLACED BY DISCUSSIONS IN "SOLAR HEATED AIR RECEIVERS"

suns (15 W/cm^2). The reradiated energy loss from the cavity is expressed through the magnitude of the cavity view factor, F_{1R2}, which is a function of the geometry of the cavity. Reradiation energy loss from the cavity could be reduced still further, if required, by increasing the depth to width ratio d/w of the example cavity from unity to say three. Such a change would reduce F_{1R2} from 0.52 to 0.28 and the reradiated energy by fifty percent.

In the following discussion, it will be assumed that the magnitude and distribution of the incremental flux to the cavity walls may be controlled, that the rear dome will receive maximum flux, and that the sides, floor and ceiling of the cavity will each receive about one third of the flux to the rear dome. Calculations of the flux distributions in the incident beams and radiation interchange view factors between the receiver surfaces and the heliostat field support these assumptions. It is also assumed that the compressed air supply is incrementally heated to the desired temperature by first passing it over the rear dome to absorb heat and then by passing it over each of the side, floor and ceiling domes where further heat inputs are absorbed.

The energy balance through the dome wall requires that incremental flux to a dome equals that conducted through the dome wall which in turn equal that removed by impingement heat transfer and absorbed by the air, i.e.,

$$\text{Incremental Flux} = \frac{K}{t}(T_1 - T_2) = h(T_2 - T_{air_{in}}) = C_P\, Q(T_{air_{out}} - T_{air_{in}}) \qquad (6)$$

where K = thermal conductivity of ceramic dome

T_1 = cavity surface temperature ~ °F

T_2 = inner dome surface temperature ~ °F

$T_{air_{out}}$ = air temperature after impingement ~ °F

$T_{air_{in}}$ = air temperature before impingement ~ °F

The performance of the five dome cavity receiver segment d/w = 1.0 was evaluated using equation 6 and the results are summarized in Table 2. In the design considered, the incoming air supply is heated to 1800°F in five stages with equal incremental air temperature rises in domes 2 through 5. Also a design is considered in which maximum (for the parameters chosen) and equal heat transfer coefficients are utilized in domes one and five and somewhat lower coefficients are used in domes 2 through 4.

The cavity operates at a temperature of 2350°F which is sufficiently high to provide the required temperature differential through the dome for conduction heat transfer and sufficiently low to utilize to advantage the high heat transfer coefficient attainable with the impingement heat transfer approach. The low cavity operating temperature results in a reradiated flux loss of only 150 suns.

The calculations summarized in Table II are for an air flow rate of 2.0 scfm/in^2 and an impingement interhole spacing of four, $x_n/_D = 4.0$. The compressed air from the ground enters at 375°F and after impingement cooling of the five domes leaves at 1800°F. The cavity receiver operates at an input level of 1740 suns which can easily be achieved by flat heliostat/central tower systems. The total impingement pressure drop for the flow through five domes is only 0.90 PSI. The 0.90 PSI pressure drop provides the head required to obtain the necessary velocity in the impingement holes but not include piping losses, if any,

Table 2. Cavity Receiver Performance (d/w = 1.0)

Item	Rear Dome	Side Dome 2	Ceiling Dome	Side Dome 2	Floor Dome	V
Q scfm/in^2	2	———	———	———	———	–
T_1 cavity temp ~ °F	2350	———	———	———	———	–
$T_{air_{in}}$ ~ °F	375	935	1151	1367	1583	–
ΔT_{air} ~ °F	560	216	216	216	216	–
$T_{air_{out}}$ ~ °F	935	1151	1376	1583	1800	–
Number of suns absorbed/dome	630	240	240	240	240	1590
h ~ BTU/ft^{2}hr°F	120	59	71	89	120	–
P ~ psi	0.18	0.18	0.18	0.18	0.18	0.90
$q_{radiation\ loss}$ ~ suns	–	–	–	–	–	150
total incident flux ~ suns	–	–	–	–	–	1740

to carry the air from one dome to the next. Other pressure drops in the system will include those required to overcome piping losses and buoyant forces as the air supply is brought to the receiver and thence back to the ground through the tower. However, calculations show that the pumping power required to overcome the buoyant forces is only one tenth of one percent of the electrical output of a plant. It should be noted that the design approach selected (Table 2) is but one of a number of possible combinations of heat transfer magnitude, cavity operating temperature, air flow rate, etc. and that other combinations of these parameters should be examined.

A receiver thermal efficiency of 91 percent is achieved with the five dome cavity receiver (see Table 3). Net receiver efficiency after subtraction of pumping power is still 91 percent and overall cycle efficiency, from reflected energy from the heliostat field to electricity, is 40 percent.

Table 3. System Efficiency

1.	Incremental flux absorbed by air	1590 suns
2.	Radiation loss 2350°F cavity operating temperature cavity, L/D = 1.0, F_{1R2} = 0.52	150 suns
3.	Total input to receiver (1 + 2)	1740 suns
4.	Receiver thermal efficiency (1 ÷ 3)	91 percent
5.	Total pumping power (5 domes) 2 scfm/in^2, x_n/D = 4.0	9 suns
6.	Net receiver thermal efficiency (1 − 5) ÷ 3	91 percent
7.	Turbine/generator efficiency (T = 1800°F, P/P_o = 4.0)	44 percent
8.	Overall cycle efficiency (6 × 7)	40 percent

Calculations for the domed cavity receiver, have shown that the heated air receiver concept is feasible and that excellent overall cycle efficiencies may be achieved. There are still a number of ways to improve receiver efficiency which have not been investigated and it can be expected that overall cycle efficiency may be increased somewhat from that shown for the example cavity receiver. However transient receiver heating situations, which will occur at sunrise and sunset and may arise during the day due to obscuration of the sun by clouds, need to be analyzed and their implications on receiver design assessed.

Testing of Heated-Air Receivers

An incident flux level of 1800 suns is required for experimental tests of heated air receivers at their operating flux level. At the present time, this flux level may be reached over receiver diameters ranging from a few inches to a few feet using solar furnaces or solar simulators. Two furnaces with this capability are the 35KW U. S. Army furnace at White Sands Missile Range (W. S. M. R.) and the 1000 KW C. N. R. S. solar furnace at Odeillo, France. The image contours[8] of these furnaces are graphed in Figure 17 and show that 1800 suns (180 W/cm^2) of nearly uniform flux may be achieved over 11 cm (4.5 inch) and 60 cm (24 inch) diameter receivers in the W. S. M. R. and C. N. R. S. furnaces, respectively. The M.I.T. Lincoln Laboratory solar simulator which employs a 7-lamp cluster of compact xenon arc lamps has the capability to provide, after minor adjustments, the required flux over an 11 cm (4.5 inch) diameter target (Fig. 15) with an exact reproduction of the terrestrial solar spectrum. Testing in a solar simulator may offer some advantages which include constancy of input flux conditions and unlimited testing duration.

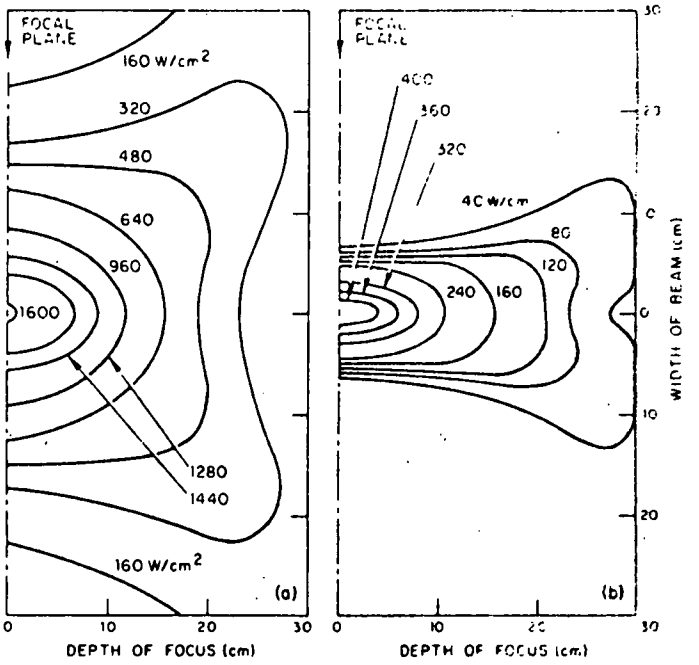

Fig. 17. Image contours in horizontal plane for (a) 1000-kw CNRS, and (b) 35-kw U. S. Army solar furnaces.

System Cost Considerations

In general, the required heliostat area for a given electrical output depends strongly on the thermal efficiency of the receiver; the higher the receiver thermal efficiency, the lower the required area. For a solar steam plant where the quoted receiver efficiency is nearly 100 percent, the heliostat costs[2] still represent about 50 percent of the total cost of the plant, while the receivers and the tower plus piping each represent an additional 10 percent of the total cost. A small change in receiver efficiency has a large effect

on total cost since it affects the major cost item of the solar plant.

Because of the preceding discussion, it is important to develop a highly efficient heated air receiver. The 5-dome/cavity receiver considered herein has an efficiency of 91 percent and is thus a worthy candidate for development.

Conclusions

Solar heated air turbine electrical generating plants are feasible and 40 percent overall efficiency appears achievable using a regenerating gas turbine cycle and a highly efficient heated-air receiver. Such a receiver, which provides 1800°F air at an overall receiver thermal efficiency of 90 percent seems feasible. High efficiency is achieved from the use of a cavity receiver in conjunction with impingement heat-transfer techniques which results in low temperature (2350°F) cavity operation and minimization of reradiation heat losses.

References

1. "Solar Thermal Power Systems Based on Optical Transmission," Progress Report 1, NSF/RANN/SE/DI-39456/PR/73/4, University of Houston and McDonnell-Douglas Astron. Co. (Feb. 15, 1974).
2. "Solar Power System and Components Research Program" NSF/RANN/SE/AER75-07570, Martin Marietta (Jan. 1975).
3. "The Turbojet Power-Pac-Packaged Electrical Generation Station," Turbo Power and Marine Systems, United Aircraft subsidiary (Mar. 1973).
4. Prof. David Wilson, MIT Mech. Eng. Dept., private communication.
5. "Solar Thermal Conversion Mission Analysis-SW United States – Comparative System/Economics Analyses," 4, ATR 74(7417-16) Aerospace Corp. (Nov. 15, 1974).
6. M. A. Krenzke and R. M. Charles, "The Elastic Buckling Strength of Spherical Glass Shells," David Taylor Model Basin Report 1759 (Sept. 1963).
7. M. Jakob, Heat Transfer, II, 54-62 (Wiley, New York, 1957).
8. Dr. J. D. Walton, Jr., Georgia Inst. of Tech., Engineering Experiment Station, private communication.

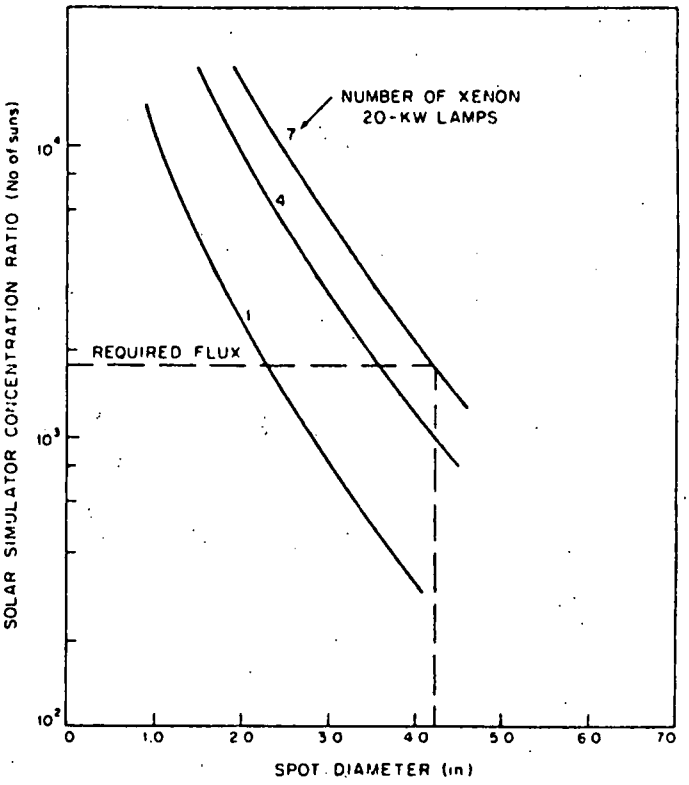

Fig. 18. Capability of M.I.T Lincoln Laboratory's multi-sun, solar simulator.